ARTICLE
Journal of Cellular Biochemistry 118:154–162 (2017)

Journal of Cellular Biochemistry

Preservation of the 3D Phenotype Upon Dispersal of Cultured Cell Spheroids Into Monolayer Cultures

Vasilij Koshkin,[1] Laurie E. Ailles,[2] Geoffrey Liu,[3] and Sergey N. Krylov[1]*

[1]*Department of Chemistry and Centre for Research on Biomolecular Interactions, York University, Toronto, Ontario, Canada M3J 1P3*

[2]*Department of Medical Biophysics, University of Toronto, Toronto, Ontario, Canada N5G 1L7*

[3]*Department of Medicine, Medical Oncology and Haematology, Princess Margaret Hospital, Toronto, Ontario, Canada M5G 2C4*

ABSTRACT

In functional cytometric studies, cultured cells are exposed to effectors (e.g., drugs), and the heterogeneity of cell responses are studied using cytometry techniques (e.g., image cytometry). Such studies are difficult to perform on 3D cell cultures. A solution is to disperse 3D clusters and transfer the cells to the 2D state before applying effectors and using cytometry. This approach requires that the lifetime of the 3D phenotype be longer than the duration of the experiment. Here we studied the dynamics of phenotype transformation from 3D to 2D and searched for means of slowing this transformation down in dispersed spheroids of MCF7 cells. We found three functional biomarkers of the 3D phenotype in MCF7 cell spheroids that are absent in the 2D cell culture: (i) the presence of a subpopulation with an elevated drug-expelling capacity; (ii) the presence of a subpopulation with an elevated cytoprotective capacity; and (iii) the accumulation of cells in the G1 phase of the cell cycle. Monitoring these biomarkers in cells transferred from the 3D state to the 2D state revealed their gradual extinction. We found that the combined application of an elevated cell density and thiol-containing medium supplements increased the lifetime of the 3D phenotype by several fold to as long as 96 h. Our results suggest that extending the lifetime of the 3D phenotype in the cells transferred from the 3D state to the 2D state can facilitate detailed functional cytometric studies, such as measurements of population heterogeneity of cytotoxicity, chemosensitivity, and radiosensitivity. J. Cell. Biochem. 118: 154–162, 2017.

KEY WORDS: CANCER; 3D CELL CULTURE; FUNCTIONAL CYTOMETRIC STUDIES; FUNCTIONAL BIOMARKERS

In cancer biology, ex situ experimental cellular models are defined as cell populations taken out of context of an in situ tumor to facilitate functional studies of cancer cells under well-controlled conditions [Piscitelli et al., 2015]. Formally, such models can be characterized by their level of cell-cell interactions which is associated with the model dimension [Katt et al., 2016]. Monolayers of cells, in which every cell can interact with several neighboring cells, but is still exposed to direct interactions with the support surface and cell media, represent a two-dimensional (2D) model. Multi-layered cells or cell spheroids, in which the majority of cells are completely surrounded by other cells, can be considered as a three-dimensional (3D) model [Maltman and Przyborski, 2010]. 3D models are more relevant to real cancer tissues than 2D models, and, therefore, they are preferable in cancer-biology studies [LaBarbera et al., 2012].

A distinct property of cancer-cell populations is their significant heterogeneity (in comparison to corresponding normal cells) [Zellmer and Zhang, 2014]. Cancer cell populations are heterogeneous with respect to their genotypes and phenotypes because of genomic instability [Heng et al., 2011]. Additional sources of cancer cell heterogeneity are hierarchical organization of tumors (tumor initiating and differentiated cells) and cell proliferation (different cell cycle phases) [Magee et al., 2012]. Many functional properties are therefore expected to vary significantly from cell to cell in cancer cell populations. Due to significant cell-to-cell variations, cancer cell populations are often studied with cytometry techniques, for example, flow cytometry, image cytometry, chemical cytometry, etc. [Hu et al., 2004; Haselgrübler et al., 2014]. Cytometry techniques provide "single-cell resolution" and can thus facilitate the identification of distinct sub-populations of cells within heterogeneous cell populations [Prince et al., 2007].

Another important aspect of cancer biology is that it often requires functional cytometric studies in which the cells are

Grant sponsor: NSERC Canada; Grant number: CHRP 462341-2014; Grant sponsor: CIHR Canada; Grant number: CPG 134747.

*Correspondence to: Sergey N. Krylov, Department of Chemistry and Centre for Research on Biomolecular Interactions, York University, Toronto, Ontario, Canada M3J 1P3. E-mail: skrylov@yorku.ca

Manuscript Received: 6 May 2016; Manuscript Accepted: 8 June 2016

Accepted manuscript online in Wiley Online Library (wileyonlinelibrary.com): 10 June 2016

DOI 10.1002/jcb.25621 • © 2016 Wiley Periodicals, Inc.

subjected to the influence of an effector (e.g., a ligand that binds a receptor on the cell surface, a drug, or a substrate of a cellular process), and the heterogeneity of cell functional responses to the effector are studied with cytometry [Simard et al., 2014]. Functional cytometric studies can be reliably performed on 2D cellular models [Pozarowski et al., 2006]. By contrast, such studies are difficult to conduct directly on 3D models because of two major limitations. First, the delivery of effectors to inner cells is hindered by outer cells surrounding them, and as a result it is difficult to achieve homogeneous delivery of the effectors to all cells in the 3D model [Mehta et al., 2012]. Second, only image cytometry (microscopy) can, in principle, be applied directly to 3D models without disturbing their homeostasis and even in this case, accurate imaging of inner cells in 3D models is affected by optical aberrations caused by outer cells [Smith et al., 2010]. Thus on the one hand, 3D models are most relevant to tumor tissues; but, on the other hand, they are not directly suitable for functional cytometric studies.

A logical solution to the problem of combining 3D cell models with functional cytometric studies is growing cells in a 3D state, disintegrating the 3D cellular clusters into individual cells, and transferring the cells to the 2D state for functional cytometric studies [Dubessy et al., 2000; Chandrasekaran et al., 2014]. After being transferred from the 3D state to the 2D state, the cells will start gradually changing their phenotype from 3D to 2D [Chua et al., 2007]. The phenotype, however, cannot change immediately, and thus the results of functional cytometric studies performed on cells transferred from the 3D to the 2D state can be associated with the 3D phenotype if the experiment is shorter than the lifetime of the 3D phenotype [Xu et al., 2014]. The situation is simple when the experiment is of the "end-point" type, for example, fast "sacrificial" analysis with flow cytometry or chemical cytometry, or the analysis of fixed cells [Olive and Durand, 1994]. In such cases, it is typically presumed that the 3D phenotype is preserved during the assay [Keithley et al., 2013]; and there has been no significant evidence that this assumption is incorrect in short-term studies. The assumption of undisturbed 3D phenotype cannot be made, however, in prolonged functional cytometric assays. These assays may require relatively lengthy incubation of the cells with effectors followed by a relatively lengthy non-sacrificial analysis by image cytometry [Xu et al., 2014]. For such assays to be conclusive and for their results be unambiguously ascribed to the 3D phenotype, it is critical to assure that the lifetime of the 3D phenotype is longer than the duration of study after transferring cells from the 3D state to the 2D state. Thus, the functional cytometric studies of cells transferred from 3D to 2D models require: (i) assessing the temporal stability of the 3D phenotype of interest in the cell type of interest after the 3D to 2D transfer; and (ii) improving this stability if needed via finding suitable conditions for maintaining the 3D phenotype in the 2D state. To the best of our knowledge, there are no experimental works in which the stability or 3D phenotype upon cell transfer to the 2D state would be quantitatively assessed or attempts to improve it would be made.

We recently conducted a functional cytometric study on MCF-7 breast cancer cells dispersed from a 3D cell culture (spheroids) and transferred to a 2D state [Koshkin et al., 2016]. The cellular function studied was multi-drug resistance (MDR) and the cytometry technique used was flow cytometry. MDR function was assessed by monitoring the efflux of a fluorescent substrate of ABC transporters from the cells. It was observed that the MDR-associated substrate efflux in cells derived from the 3D model remained different from the efflux in cells derived from the 2D model for 12 h after dispersing the original cell cultures. This fact allowed us to characterize energy support of MDR-associated efflux in a 3D model and propose potential therapeutic steps to MDR suppression. The 12-h stability of the 3D phenotype suggests that dispersed cells derived from 3D clusters can be used for more clinically relevant studies such as drug-efficiency prediction and cancer subtyping. Such studies, however, may involve assays which require cells in a 2D state and are longer than 12 h (e.g., assays for cytotoxicity, chemo- and radio-sensitivity). It is therefore important to understand if the stability of the 3D phenotype of cells derived from spheroids and transferred to the 2D state can be extended beyond 12 h.

In this work, we characterized in greater detail functional features of 3D spheroid-derived cells and the dissipation of the 3D phenotype after spheroid dispersal and cell transfer to the 2D state (Fig. 1). As a control, we used cells obtained by the dispersal of a 2D cell culture. One of the most widely used cancer cell types, the MCF-7 breast cancer cell line, was employed here. We found that the 3D phenotype differs from the 2D phenotype by more heterogeneous distributions of drug-extruding and cytoprotective capacities as well as by the prevalence of the G1 phase of the cell cycle. These features were considered as a tentative functional 3D phenotype of MCF-7 cell spheroids. It was found that this phenotype can be made stable for 96 h upon culturing the dispersed cells in the 2D state by using an elevated seeding cell density and a thiol-supplemented medium. Our findings suggest that relatively lengthy functional cytometric studies (such as studies of cytotoxicity, chemo- and radio-sensitivity) can be reliably conducted on cells transferred from the 3D state to the 2D state.

MATERIALS AND METHODS

CELL CULTURE AND CHEMICALS

MCF-7 human breast cancer cells were obtained from the American Type Culture Collection (ATCC, Manassas, VA) and maintained (as recommended by ATCC) by culturing them in monolayers in DMEM medium containing 10% FBS and 1% penicillin/streptomycin. The 3D culture protocol for generation of spheroids (100–150 μm in diameter) was adapted from elsewhere [Olea et al., 1992; Ho et al., 2011; Chandrasekaran et al., 2012]. Briefly, cells grown in a monolayer where harvested and seeded onto 6-well plates coated with 1% (w/v) agar (3×10^5 cells/well) and cultured for 2 days in MammoCult basal medium with appropriate supplements (cat # 05621 and 05622, STEMCELL Technologies, Inc., Vancouver, BC, Canada). Typical images of spheroids and monolayers are shown in Figure 2. For functional cytometric studies, spheroids were dispersed into individual cells by a treatment with a trypsin/EDTA mixture (0.05%). The dispersed cells were assayed either immediately after dispersal or upon culturing them in a 2D state (monolayer) for various periods of time. All cultures were grown at 37°C in a humidified atmosphere of 5% CO_2.

Cell culture reagents were purchased from Gibco BRL (Grand Island, NY). *N*-Acetyl-D-cysteine (D-NAC) was obtained from

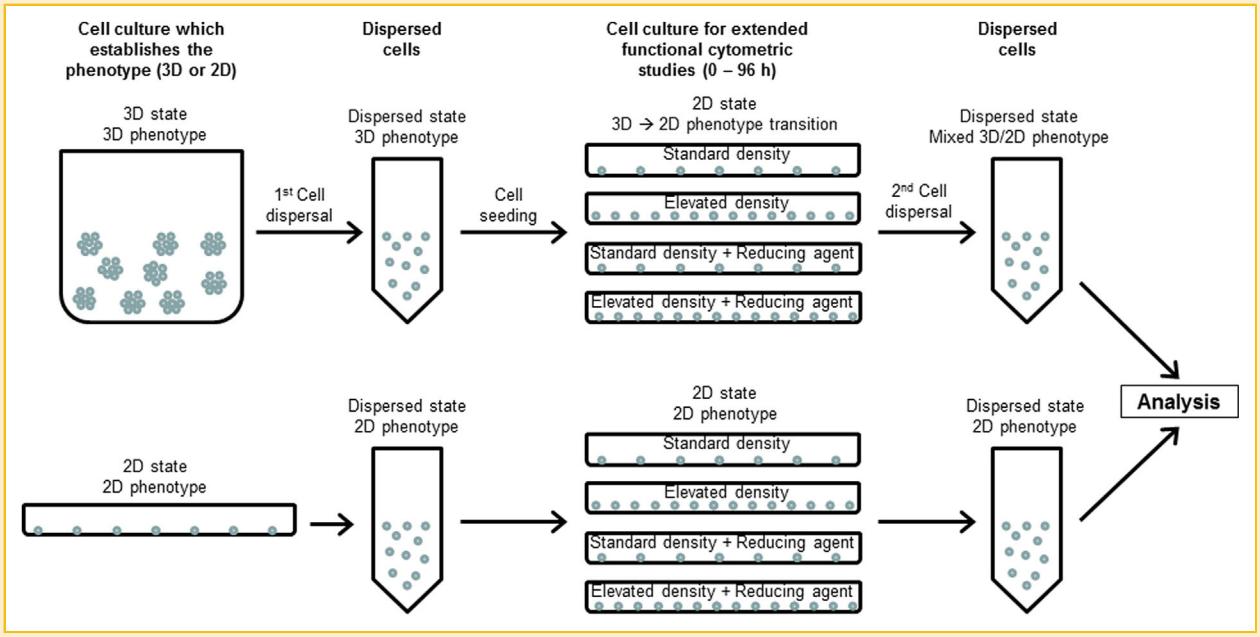

Fig. 1. A simplified schematic of the experimental study conducted in this work.

Research Organics (Cleveland, OH). All other chemicals were sourced from Sigma–Aldrich (Oakville, Ontario).

FLOW CYTOMETRY MEASUREMENT OF MDR TRANSPORT AND AlDH ACTIVITY

MDR efflux and activity of a cytoprotective enzyme (aldehyde dehydrogenase, AlDH) were determined in a combined assay using a sequential protocol reported elsewhere [Pearce and Bonnet, 2007]. First, the MDR efflux assay was performed by loading cells with an MDR substrate (mitoxantrone) with (w/) or without (w/o) an MDR inhibitor (cyclosporin), essentially as detailed earlier [Koshkin et al., 2016]. Cells were allowed to accumulate mitoxantrone for 30 min w/ or w/o the negative contribution of MDR counter-transport (depending on the presence of MDR inhibitor). Afterwards, the cells were kept on ice for 30 min for blocking MDR transport, washed twice with ice-cold Ca-/Mg-free PBS and subjected to the AlDH activity assay (Aldefluor kit) according to the recommendations of the manufacturer (Stem Cell Technologies, Vancouver, BC, Canada). Cells were suspended in the Aldefluor buffer supplemented with the MDR inhibitor (cyclosporin) to block further functioning of MDR transporters. Cells were supplied with either AlDH substrate (BODIPY-aminoacetaldehyde, BAAA), or a combination of BAAA and an AlDH inhibitor (diethylaminobenzaldehyde, DEAB). The AlDH reaction was allowed to proceed for 30 min at 37°C; cells were washed in cold Ca/Mg-free PBS and analysed for the accumulated MDR substrate and the formed AlDH product by flow cytometry

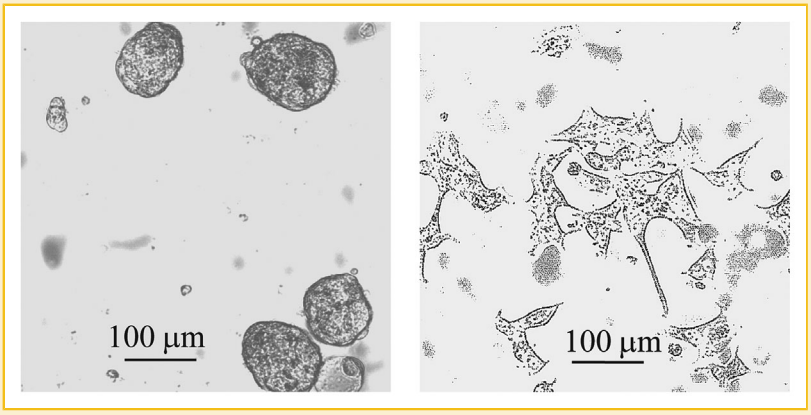

Fig. 2. Typical images of 3D spheroids (left) and 2D cell clusters (right) formed by MCF-7 cells.

(BD FACSCanto II flow cytometer, BD Biosciences, San Jose, CA). The MDR substrate (mitoxantrone) was measured using the FL3 channel with excitation at 635 nm and detection through a 670 nm long-pass emission filter. The AlDH product was measured using the FL1 channel with excitation at 488 nm and detection through a 515–545 bandpass filter. Data were recorded in FCS3 format, fluorescence of the unstained cells was set within the first log decade, and dead cells were excluded by propidium iodide (2 μM) staining. The interference between fluorescence of different fluorophores was insignificant under the experimental conditions used.

ANALYSIS OF MDR TRANSPORT AND AIDH ACTIVITY

Activities of MDR transport and AlDH reactions were determined from cell population distributions of accumulated MDR substrate and formed AlDH product. To account for non-specific signal, distributions within cells with inhibited MDR/AlDH (negative control) and naive cells were compared. In the case of MDR it was performed through subtraction of univariate histograms as was described in detail elsewhere [Koshkin et al., 2016]. The distribution of MDR substrate within spheroid cells (in contrast to monolayer cells) is bimodal, reflecting the occurrence of a minor subpopulation with a high rate of MDR efflux (termed "high drug efflux cancer cells," HDECC, [Xia et al., 2010]) and a major subpopulation with a marginal rate of MDR efflux. A differential histogram resulting from the subtraction (test population MDR_{active}—control population $MDR_{blocked}$) represents the minor HDECC subpopulation only (Fig. 3A, solid traces). The normalized area of the histogram peak characterizes abundance of the HDECC subpopulation.

The AlDH reaction was analyzed by comparison of bivariate cytograms of AlDH product fluorescence vs side scatter, according to recommendations of the AldeFluor kit manufacturer (Stem Cell Technologies, Vancouver, BC, Canada). To detect cells with AlDH activity (AlDH-positive cells, $AlDH^+$) flow cytometric gate excluding AlDH-negative ($AlDH^-$) cells was established using cells treated with AlDH inhibitor (DEAB) (Fig. 3B, left panels). Upon application of this gate to uninhibited cells, $AlDH^+$ cells fall within the gate (Fig. 3B, right panels).

FLOW CYTOMETRY ANALYSIS OF CELL CYCLE

Cell phases in the cell cycle were determined from cell DNA content [Tagg et al., 2008]. Cells were fixed and permeabilized with 70% cold ethanol and treated with RNaseA (10 μg/mL) and propidium iodide (400 μg/mL) (30 min, 37°C). DNA content was determined by flow cytometry in the Fl3 channel with excitation at 488 nm and detection through a 670 nm long-pass emission filter; data analysis was performed using FlowJo software.

2D CULTURING OF DISSOCIATED SPHEROID CELLS

Figure 1 shows the major experimental steps. For 2D culturing of cells derived from the 3D cell culture, the spheroids were dispersed to single cells with trypsin-EDTA treatment (0.05% trypsin-EDTA for 5 min) as described elsewhere [Morrison et al., 2012]. The dispersed cells were plated onto standard dishes and cultured for different times with daily changes of the culture medium. For control purposes, the cells derived from a 2D cell culture were studied. A cell monolayer was dispersed with the above-mentioned trypsin-EDTA treatment. The cells derived from the dispersal of the 2D culture were plated, cultured and analysed in parallel with spheroid-derived cells. The effect of cell density on the cultured cells' phenotype was examined by comparing cells seeded either at a standard density recommended by the American Type Culture Collection (ATCC) or at

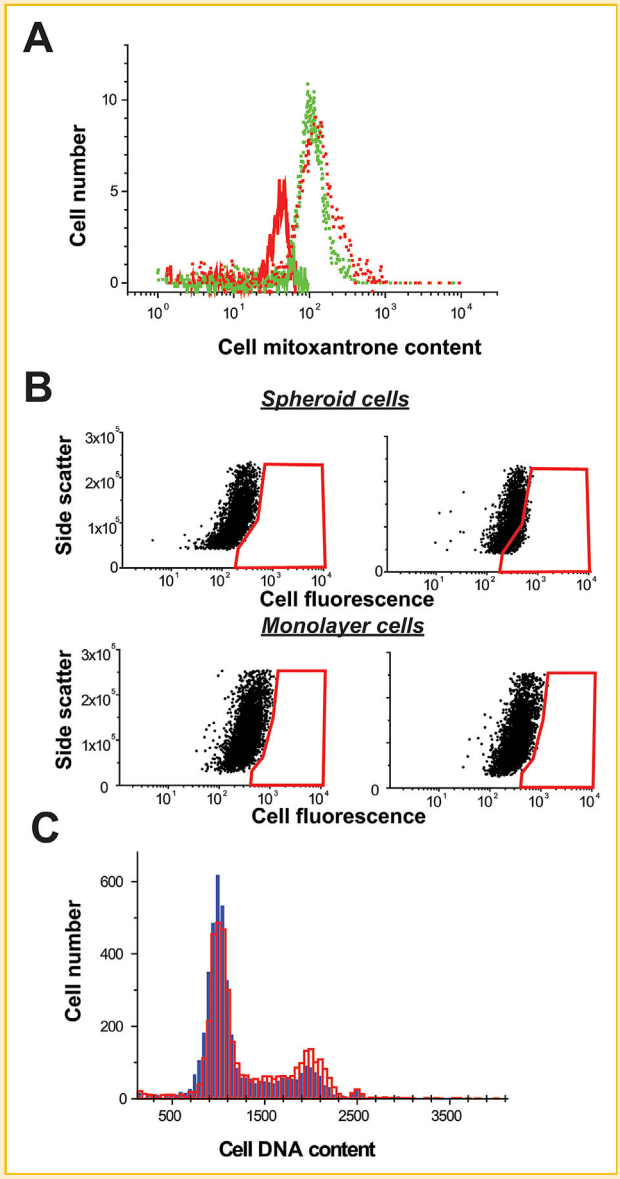

Fig. 3. Comparative cytograms of MDR capacity (A), AlDH activity (B), and the cell cycle profile (C) in 3D- and 2D-cultured cells. Panel A: the presence of an HDECC subpopulation in 3D but not 2D cells is demonstrated by differential (MDRactive minus MDRblocked) histograms of accumulation of the MDR substrate (the red solid trace corresponds to the 3D model, the green solid trace corresponds to the 2D model, and the dotted traces show total populations). Panel B: Cell fluorescence is plotted vs side scatter in spheroid- and monolayer-derived cells. Gates (red polygons) excluding the $AlDH^-$ population were established using cells with inhibited AlDH (negative control, left panels); upon their application to the test cells (right panels), the gates incorporate a cell fraction with high AlDH-dependent fluorescence. Panel C: cell cycle profiles in 3D-derived cells (blue filled histogram) and 2D-derived cells (red empty histogram).

a doubled standard density (further increase in seeding density caused significant cell death during culturing periods longer than 24 h). Redox modulation of the cultured cells' phenotype was studied by supplementation of culture medium with redox modulators specified in the Results section and figure legends.

RESULTS

CHARACTERISTIC FUNCTIONAL MARKERS OF MCF-7 CELLS IN 3D CULTURE AND THEIR LOSS AFTER TRANSFER TO THE 2D STATE

We have found recently that 3D culturing of MCF-7 cells induces the appearance of a cell subpopulation with an elevated drug efflux (high drug efflux cancer cells—HDECC) [Koshkin et al., 2016], capable of promoting drug resistance in MCF-7 spheroids. The present study aims at a broader functional characterization of these 3D-grown breast cancer cells, for which the MDR activity assay was supplemented with such clinically important cell parameters as their cytoprotective capacity (represented by the activity of a key enzyme, aldehyde dehydrogenase, AlDH) and progression through the cell cycle. The examination of cells from freshly dissociated spheroids confirmed the presence of the HDECC subpopulation of a size similar to that previously found (Fig. 3A). In addition, measurements of AlDH activity revealed the presence of an AlDH-positive cell fraction ($AlDH^+$) at a level of ~5% of the total cell count (Fig. 3B). Finally, the cell cycle analysis showed cell accumulation in the G1 phase (Fig. 3C). Thus, the presence of HDECC and $AlDH^+$ subpopulations and the greater proportion of cells in G1 phase could be considered as a tentative 3D-specific phenotype of MCF-7 cells. However, these 3D-specific markers gradually disappear with different rates in the course of culturing the 3D-derived cells in the 2D state (Figs. 4–6); this limits the time frame for experimentation with such cells from the time of dispersal of the 3D culture to the time when the 3D phenotype significantly decays. This fact prompted us to search for means to stabilize the 3D phenotype after dispersal of 3D spheroids and transfer the dispersed cells to the 2D state.

CELL DENSITY MODULATION AND 3D PHENOTYPE

An immediate effect of the cell transfer from 3D spheroid to the 2D monolayer is a dramatic reduction in the extent of cell-cell connections. The extent of cell-cell contact in a monolayer is determined by cell density, which, therefore, has a variety of consequences for cell physiology [Boumédiene et al., 2001; Dupre-Crochet et al., 2007; Tophkhane et al., 2009]. One can expect that elevated cell density increases the level of cell-cell contact and can thus favor the preservation of the 3D phenotype in dissociated spheroid cells. To test this hypothesis the dispersed spheroid cells were seeded at a standard seeding density recommended by ATCC (4×10^4 cells/cm^2) and at a doubled standard density (8×10^4 cells/cm^2) and cultured in parallel. Then the presence of the HDECC and $AlDH^+$ subpopulations as well as the distribution of cells in the cell cycle were examined. Figure 5 shows loss of the HDECC subpopulation upon 2D culturing of dispersed spheroid cells and indicates that this loss is significantly slowed down at the elevated cell density. By contrast, as shown in Figure 5, the disappearance of the $AlDH^+$ subpopulation (the 2nd 3D-specific marker) proceeds similarly at the standard and elevated seeding densities of cultured cells. Finally, the 3D-specific cell cycle distribution, along with the HDECC subpopulation, could be preserved during 2D culturing by elevation of the cell density (Fig. 6).

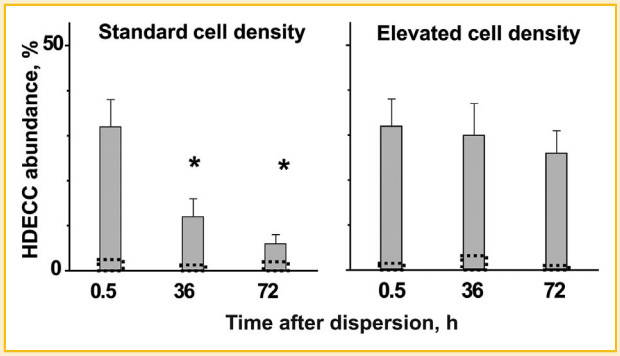

Fig. 4. The influence of the seeding cell density (standard of 4×10^4 or elevated of 8×10^4 cells/cm^2) on the loss of the HDECC subpopulation in the course of 2D culturing of spheroid-derived cells. Overlaid dotted bars represent the negligible HDECC content in the control culture derived from the dispersed 2D cell culture. An asterisk denotes statistical significance (at the $P < 0.05$ level) of the difference between HDECC abundance after either spheroid dispersion (0.5 h) or dispersion followed by 2D cell culturing (36 and 72 h).

REDOX BALANCE MODULATION AND ALDH$^+$ CELLS

The fact that elevated seeding cell density provides only partial preservation of the 3D phenotype prompted us to consider other effects of spheroid dispersal on its constituent cells. Obviously, cells released from 3D spheroids become more prone to exposure to environmental factors, in particular, to oxygen. Increased oxygenation of the dispersed cells can make them more susceptible to oxidative stress. Therefore, the maintenance of dispersed cells in the medium with the redox balance shifted toward reduction might

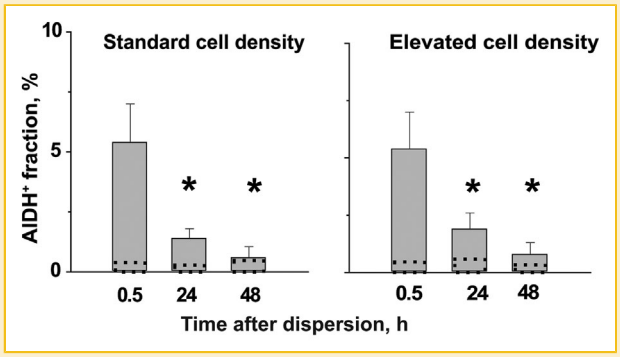

Fig. 5. The influence of seeding cell density (standard of 4×10^4or elevated of 8×10^4 cells/cm^2) on the loss of the $AlDH^+$ subpopulation during the course of 2D culturing of spheroid-derived cells. The overlaid dotted bars correspond to a very small $AlDH^+$ subpopulation during the 2D culturing of monolayer-derived cells. Asterisks denote statistical significance (at the $P < 0.05$ level) of the difference between the $AlDH^+$ fraction after either spheroid dispersion (0.5 h) or dispersion followed by 2D cell culturing (24 and 48 h).

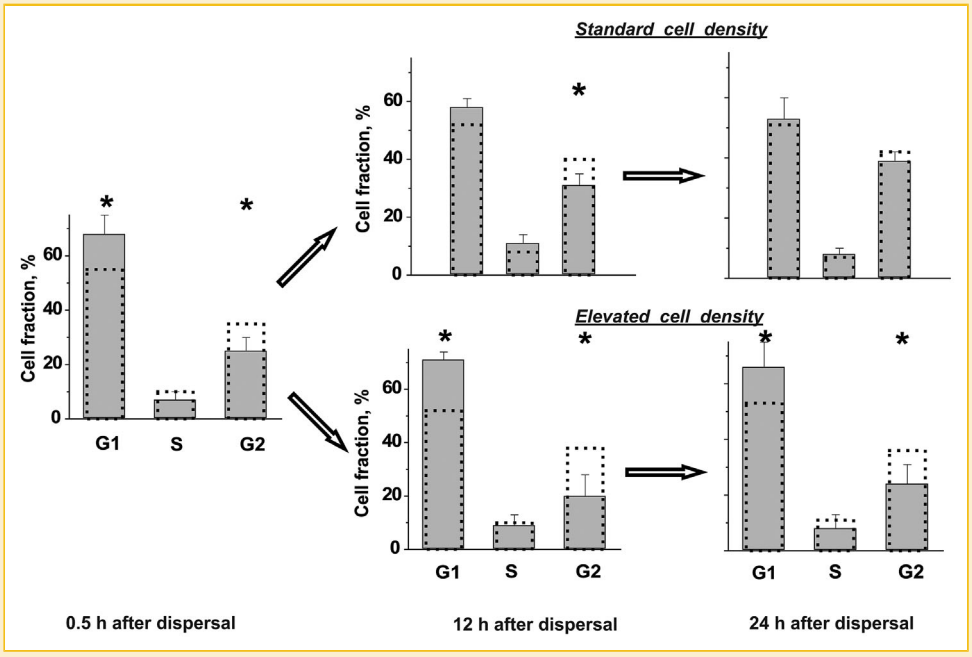

Fig. 6. The influence of the seeding cell density (standard of 4×10^4 or elevated of 8×10^4 cells/cm^2) on 3D-specific cell distribution between cell cycle phases (prevalence of the G1 phase) during the course of 2D culturing of spheroid-derived cells. The overlaid dotted bars represent cell distribution between cell cycle phases in the parallel control culture of monolayer-derived cells. An asterisk denotes statistical significance (at the $P < 0.05$ level) of the difference between monolayer- and spheroid-derived cultures.

contribute to extended life of the 3D phenotype, in particular, it can potentially prevent the loss of the AlDH$^+$ subpopulation. To test this hypothesis, we supplemented the growth medium of dispersed spheroid cells with the principal cellular reducing agent, glutathione (GSH, 5 mM). The addition of GSH produced no significant effect on the dynamics of the AlDH$^+$ subpopulation in dispersed spheroid cells seeded at the standard density. However, cells seeded at the elevated cell density responded to the GSH supplement with a pronounced lifetime extension of the AlDH$^+$ subpopulation (Fig. 7A) (increasing GSH supplement to 10 mM did not lead to further extension of AlDH$^+$ lifetime). Thus, the combined application of the elevated seeding cell density and GSH produced a synergistic favorable effect on this part of the 3D phenotype.

Further, the possibility of similar effects exerted by other antioxidant agents was tested. Ascorbic acid, tocopherol, Trolox, *N*-acetyl-L-cysteine (L-NAC) and *N*-acetyl-D-cysteine (D-NAC) were added to the cell media at concentrations commonly used with this type of cells (specified in a legend to Fig. 7). Figure 7B, shows that only L- and D-NAC provided appreciable protection for the AlDH$^+$ subpopulation. The lack of interchangeability between thiol-containing (GSH and NAC′s) and other reducing agents allows us to ascribe this protection to thiol-mediated mechanisms rather than non-specific antioxidant effects. Next, considering potential targets of thiol reagents, it is important that GSH and L-NAC are poor cell permeants. Thus, they need to be enzymatically hydrolyzed into cysteine to be able to enter the cell and exert an intracellular effect; otherwise, their action is considered to be confined to extracellular targets [Pocernich and Butterfield, 2012; Samuni et al., 2013]. Therefore, the protective effect provided by the D-stereomer of NAC, which is not susceptible to enzymatic hydrolysis, suggests mostly extracellular action of thiols in this system. Apparently, the maintenance of extracellular thiol groups in the reduced state is required for the stabilization of the 3D phenotype under consideration.

OVERALL LONG-TERM MAINTENANCE OF THE 3D PHENOTYPE UNDER 2D CONDITIONS

Monitoring dynamics of each individual 3D phenotype marker allowed us to determine factors capable of extending lifetimes of these markers under 2D culturing conditions. As the next step, a comprehensive characterization of the entire phenotype on an extended time scale was performed. Single cell suspensions obtained from dispersed spheroids were divided into samples analyzed either immediately or after 96 h of 2D culturing under various conditions. A culture period of 96 h covers time periods commonly employed in chemosensitivity assays [Sumantran, 2011]. Phenotypes consisting of three parameters can be conveniently presented as points in a three-dimensional graph with axes corresponding to abundances of HDECC, AlDH$^+$ and G1 subpopulations (Fig. 8). The three-dimensional diagram shows that 96 h of 2D culturing of spheroid-derived cells leads to a profound loss of the 3D phenotype under standard conditions. The separate use of the elevated seeding cell density or GSH as a cell-medium supplement led to marginal phenotype preservation. The combined application of the elevated cell density and GSH preserves the 3D phenotype in the dissociated spheroid cells for at least 96 h (Fig. 8). Thus, the synergistic action of the elevated cell density and extracellular thiols holds for entire 3D phenotype on an extended time scale.

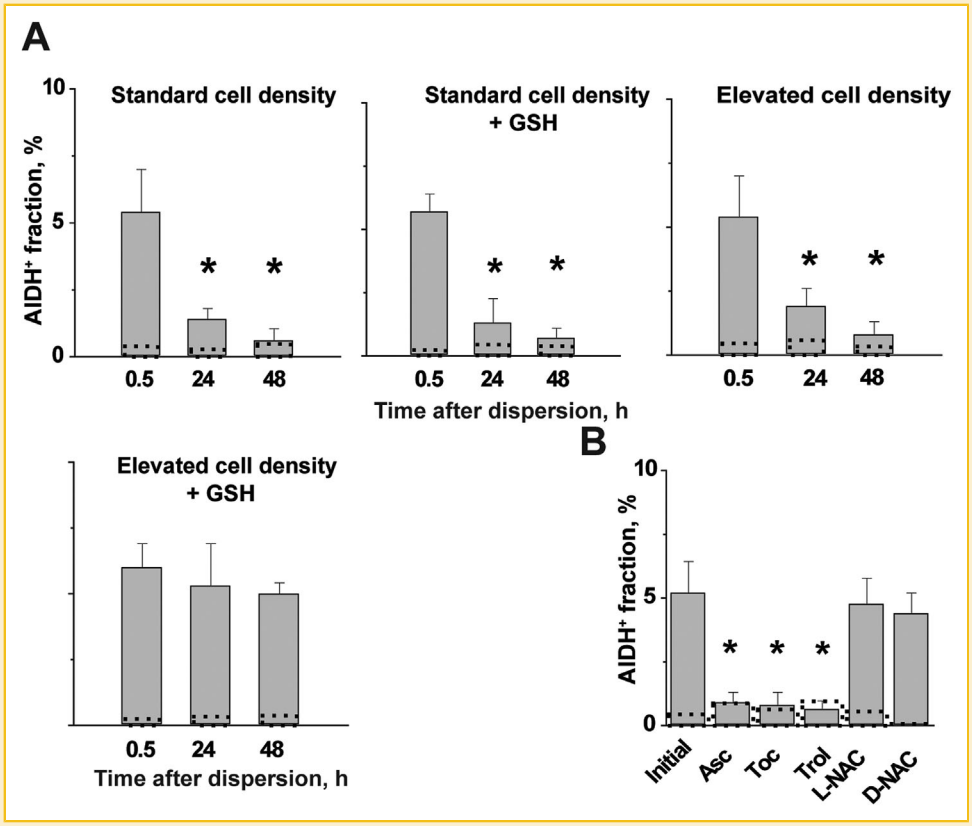

Fig. 7. The combined effect of cell density and presence of a reducing agent on the loss of the AlDH$^+$ subpopulation during the course of 2D culturing of spheroid-derived cells. Panels A compare individual effects of the elevated seeding cell density and the presence of GSH supplement (5 mM) in the cell medium with their synergistic effect. Panel B compares the efficiency of other redox-active supplements. "Initial" shows the size of the AlDH$^+$ fraction 0.5 h after dispersion while the rest of experiments correspond to 48 h 2D culturing at the elevated seeding cell density in media supplemented with: 4 mM ascorbic acid 2-phosphate (Asc), 30 μM tocopherol (Toc), 30 μM Trolox (Trol), 4 mM *N*-acetyl-L-cysteine (L-NAC), and 4 mM *N*-acetyl-D-cysteine (D-NAC). The overlaid dotted bars correspond to a very small AlDH$^+$ subpopulation during the 2D culturing of monolayer-derived cells. Asterisks denote a statistically significant (at the $P < 0.05$ level) decrease of the AlDH$^+$ subpopulation after spheroid dispersion.

DISCUSSION

The application of functional cytometric studies to multicellular 3D cell clusters requires either retrieval of the single cell signal from within the multicellular cluster or cluster dispersion to single cells. Of the various cytometric methods, 3D microscopy is best suited for retrieval of optical signal from the single cluster cells. However, despite impressive progress in 3D microscopy, studying entire cell clusters is associated with significant difficulties [Robertson et al., 2010; Vinci et al., 2012]. Besides the pronounced deterioration of optical signal from cells located inside the cluster, the delivery of fluorescent probes as well as metabolic substrates and modulators into the cluster interior space is hindered. These two factors make quantitative description of processes within 3D models highly challenging and call for approaches which can keep 3D-specific cell features for long periods after dispersal of the 3D cell clusters.

The formation of HDECC and AlDH$^+$ subpopulations and elevation in the G1 subpopulation appear to be markers of the 3D phenotype in MCF-7 cells. This 3D phenotype resembles 3D-associated features observed in some other cell types [Durand, 1990; Smart et al., 2013; Chandrasekaran et al., 2014]. Thus, our findings strengthen previous results and suggest a general character of the observed distinctions between 3D and 2D states.

Factors affecting cells in 3D culture (and lacking in 2D culture) are of two types. The first one is a cell's interactions with its immediate neighbors and the extracellular matrix, which can be considered in the first approximation as being uniform across the spheroid. The second one is diffusion limitations imposed by the whole multicellular cluster on the supply and removal of metabolites in the majority of constituent cells. This factor is increasing from the periphery to the center of a spheroid. At present, we were focusing on the phenotypic consequences of the first factor as a more general phenomenon. The limited size of spheroids used in this work (below 200 μm) makes the effect of metabolic gradients on cell functioning insignificant [Hirschhaeuser et al., 2010].

On the one hand, 3D-derived cells placed into the 2D state experience dramatically fewer cell-cell and cell-extracellular matrix interactions. On the other hand, they experience increased exposure to the environmental factors, in particular, oxygen. Though moderate hypoxia characteristic of small spheroids (at ~100 μm depth) does not suppress significantly cell metabolism [Hirschhaeuser et al., 2010; Zhou et al., 2013], it can affect redox sensitive cellular parameters. For instance, the redox potential

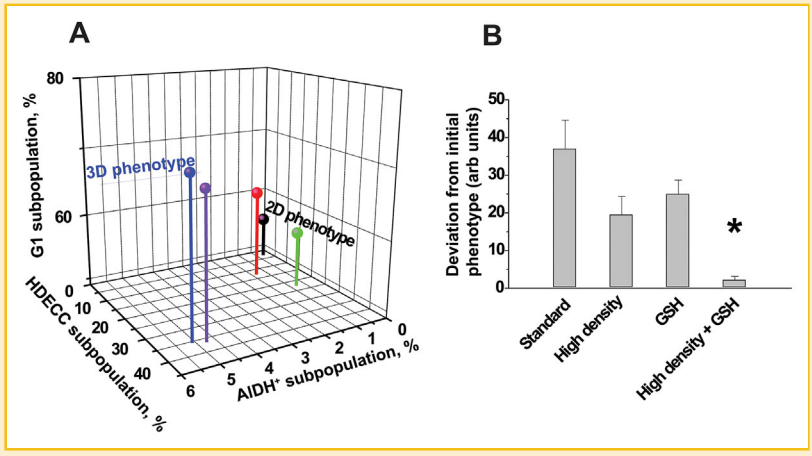

Fig. 8. Long-term protection of the 3D phenotype of spheroid-derived cells upon their transfer to the 2D state and culturing under 2D conditions. Panel A: Cell phenotypes consisting of three parameters are visualized in a corresponding three-dimensional graph. The blue symbol corresponds to cells analyzed soon (0.5–1 h) after spheroid dispersal. The black symbol corresponds to cells analyzed after 96 h of 2D culturing under standard conditions: standard seeding cell density of 4×10^4 cells/cm^2 and no reducing agent added. The red symbol corresponds to cells analyzed after 96 h of 2D culturing with an elevated seeding cell density of 8×10^4 cells/cm^2 and no reducing agent added. The green symbol corresponds to cells analyzed after 96 h of 2D culturing with a standard seeding cell density of 4×10^4 cells/cm^2 in the cell medium supplemented with GSH (5 mM). The violet symbol corresponds to cells analyzed after 96 h of 2D culturing with the combined application of the elevated cell density (8×10^4 cells/cm^2) and GSH (5 mM). Panel B: The influence of culturing conditions on the deviation of the 3D phenotype from its state after 96 h of 2D culturing. The deviation was calculated as the distance in the three-dimensional space shown in Panel A: $D = \sqrt{\Delta x^2 + \Delta y^2 + \Delta z^2}$. An asterisk denotes lack of significant ($P < 0.05$) deviation from 3D phenotype.

determined with SERS techniques in MCF-7 spheroids was found to be more negative than that in the monolayer culture [Jamieson et al., 2015]. It seems plausible that relative hyperoxygenation of spheroid cells after dispersal can be counteracted with thiol supplementation. Thus, perturbations in cell-cell interactions and redox environment can account for the functional distinctions between 3D- and 2D-derived cells and synergistic protection of 3D phenotype reported here.

Obviously, the rate of transition from the 3D phenotype to the 2D one is highly variable. In some cases, cells revert to 2D-specific functioning almost immediately after cluster dispersion [Vardimon et al., 1988; Freyer and Schor, 1989]. In other cases, the 3D-derived cells show distinctions from 2D cells for longer than a week after cluster disaggregation [Guo et al., 2014]. Our data suggest that dynamics of phenotype transition from 3D to 2D needs to be assessed in every specific case. They also demonstrate the usefulness of a search for conditions that can preserve the 3D phenotype when performing long-term assays on dispersed 3D cancer models. In particular, the 3D phenotype of dispersed breast cancer spheroids can be preserved by culturing cells at an elevated seeding cell density in medium supplemented with thiol-containing agents.

REFERENCES

Boumédiene K, Takigawa M, Pujo JP. 2001. Cell density-dependent proliferative effects of transforming growth factor (TGF)-beta 1, beta 2, and beta 3 in human chondrosarcoma cells HCS-2/8 are associated with changes in the expression of TGF-beta receptor type I. Cancer Invest 19:475–486.

Chandrasekaran S, Geng Y, DeLouise LA, King MR. 2012. Effect of homotypic and heterotypic interaction in 3D on the E-selectin mediated adhesive properties of breast cancer cell lines. Biomaterials 33:9037–9048.

Chandrasekaran S, Marshall JR, Messing JA, Hsu JW, King MR. 2014. TRAIL-mediated apoptosis in breast cancer cells cultured as 3D spheroids. PLoS ONE 9:e111487.

Chua HL, Bhat-Nakshatri P, Clare SE, Morimiya A, Badve S, Nakshatri H. 2007. Chronic NF-kappaB represses E-cadherin expression and enhances epithelial to mesenchymal transition of mammary epithelial cells: Potential involvement of ZEB-1 and ZEB-2. Oncogene 26:711–724.

Dubessy C, Merlin JM, Marchal C, Guillemin F. 2000. Spheroids in radiobiology and photodynamic therapy. Crit Rev Oncol Hematol 36:179–192.

Dupre-Crochet S, Figueroa A, Hogan C, Ferber EC, Bialucha CU, Adams J, Richardson EC, Fujita Y. 2007. Casein kinase 1 is a novel negative regulator of E-cadherin-based cell-cell contacts. Mol Cell Biol 27:3804–3816.

Durand RE. 1990. Multicell spheroids as a model for cell kinetic studies. Cell Tissue Kinet 23:141–159.

Freyer JP, Schor PL. 1989. Regrowth kinetics of cells from different regions of multicellular spheroids of four cell lines. J Cell Physiol 138:384–392.

Guo L, Zhou Y, Wang S, Wu Y. 2014. Epigenetic changes of mesenchymal stem cells in three-dimensional (3D) spheroids. J Cell Mol Med 18:2009–2019.

Haselgrübler T, Haider M, Ji B, Juhasz K, Sonnleitner A, Balogi Z, Hesse J. 2014. High-throughput, multiparameter analysis of single cells. Anal Bioanal Chem 406:3279–3296.

Heng HH, Stevens JB, Bremer SW, Liu G, Abdallah BY, Ye CJ. 2011. Evolutionary mechanisms and diversity in cancer. Adv Cancer Res 112:217–253.

Hirschhaeuser F, Menne H, Dittfeld C, West J, Mueller-Klieser W, Kunz-Schughart LA. 2010. Multicellular tumor spheroids: An underestimated tool is catching up again. J Biotechnol 148:3–15.

Ho JH, Chen YF, Ma WH, Tseng TC, Chen MH, Lee OK. 2011. Cell contact accelerates replicative senescence of human mesenchymal stem cells independent of telomere shortening and p53 activation: Roles of Ras and oxidative stress. Cell Transplant 20:1209–1220.

Hu K, Zarrine-Afsar A, Ahmadzadeh H, Krylov SN. 2004. Single-cell analysis by chemical cytometry combined with fluorescence microscopy. Instrum Sci Technol 32:31–41.

Jamieson LE, Bell AP, Harrison DJ, Campbell CJ. 2015. Monolayer to MTS: Using SEM, HIM, TEM and SERS to compare morphology, nanosensor uptake and redox potential in MCF7 cells. Proc SPIE 9531:95311I–95311I.

Katt ME, Placone AL, Wong AD, Xu ZS, Searson PC. 2016. In vitro tumor models: Advantages, disadvantages, variables, and selecting the right platform. Front Bioeng Biotechnol 4:12.

Keithley RB, Weaver EM, Rosado AM, Metzinger MP, Hummon AB, Dovichi NJ. 2013. Single cell metabolic profiling of tumor mimics. Anal Chem 85:8910–8918.

Koshkin V, Ailles LE, Liu G, Krylov SN. 2016. Metabolic suppression of a drug-resistant subpopulation in cancer spheroid cells. J Cell Biochem 117:59–65.

LaBarbera DV, Reid BG, Yoo BH. 2012. The multicellular tumor spheroid model for high-throughput cancer drug discovery. Expert Opin Drug Discov 7:819–830.

Magee JA, Piskounova E, Morrison SJ. 2012. Cancer stem cells: Impact, heterogeneity, and uncertainty. Cancer Cell 21:283–296.

Maltman DJ, Przyborski SA. 2010. Developments in three-dimensional cell culture technology aimed at improving the accuracy of in vitro analyses. Biochem Soc Trans 38:1072–1075.

Mehta G, Hsiao AY, Ingram M, Luker GD, Takayama S. 2012. Opportunities and challenges for use of tumor spheroids as models to test drug delivery and efficacy. J Control Release 164:192–204.

Morrison BJ, Hastie ML, Grewal YS, Bruce ZC, Schmidt C, Reynolds BA, Gorman JJ, Lopez JA. 2012. Proteomic comparison of MCF-7 tumoursphere and monolayer cultures. PLoS ONE 7:e52692.

Olea N, Villalobos M, Ruiz de Almodovar JM, Pedraza V. 1992. MCF-7 breast cancer cells grown as multicellular spheroids in vitro: Effect of 17 beta-estradiol. Int J Cancer 50:112–117.

Olive PL, Durand RE. 1994. Drug and radiation resistance in spheroids: Cell contact and kinetics. Cancer Metastasis Rev 13:121–138.

Pearce DJ, Bonnet D. 2007. The combined use of Hoechst efflux ability and aldehyde dehydrogenase activity to identify murine and human hematopoietic stem cells. Exp Hematol 35:1437–1446.

Piscitelli E, Cocola C, Thaden FR, Pelucchi P, Gray B, Bertalot G, Albertini A, Reinbold R, Zucchi I. 2015. Culture and characterization of mammary cancer stem cells in mammospheres. Methods Mol Biol 1235:243–262.

Pocernich CB, Butterfield DA. 2012. Elevation of glutathione as a therapeutic strategy in Alzheimer disease. Biochim Biophys Acta 1822:625–630.

Pozarowski P, Holden E, Darzynkiewicz Z. 2006. Laser scanning cytometry. In: Taatjes DJ, Mossman BT, editors. Methods mol biol v. 319. New Jersey: Humana Press. pp 165–192.

Prince ME, Sivanandan R, Kaczorowski A, Wolf GT, Kaplan MJ, Dalerba P, Weissman IL, Clarke MF, Ailles LE. 2007. Identification of a subpopulation of cells with cancer stem cell properties in head and neck squamous cell carcinoma. PNAS USA 104:973–978.

Robertson FM, Ogasawara MA, Ye Z, Chu K, Pickei R, Debeb BG, Woodward WA, Hittelman WN, Cristofanilli M, Barsky SH. 2010. Imaging and analysis of 3D tumor spheroids enriched for a cancer stem cell phenotype. J Biomol Screen 15:820–829.

Samuni Y, Goldstein S, Dean OM, Berk M. 2013. The chemistry and biological activities of N-acetylcysteine. Biochim Biophys Acta 1830:4117–4129.

Simard C, Cloutier M, Néron S. 2014. Feasibility study: Phosphospecific flow cytometry enabling rapid functional analysis of bone marrow samples from patients with multiple myeloma. Cytometry B Clin Cytom 86: 139–144.

Smart CE, Morrison BJ, Saunus JM, Vargas AC, Keith P, Reid L, Wockner L, Askarian-Amiri M, Sarkar D, Simpson PT, Clarke C, Schmidt CW, Reynolds BA, Lakhani SR, Lopez JA. 2013. In vitro analysis of breast cancer cell line tumourspheres and primary human breast epithelia mammospheres demonstrates inter- and intrasphere heterogeneity. PLoS ONE 8:e64388.

Smith LE, Smallwood R, Macneil S. 2010. A comparison of imaging methodologies for 3D tissue engineering. Microsc Res Tech 73:1123–1133.

Sumantran VN. 2011. Cellular chemosensitivity assays: An overview. Methods Mol Biol 731:219–236.

Tagg SLC, Foster PA, Leese MP, Potter BVL, Reed MJ, Purohit A, Newman SP. 2008. 2-Methoxyoestradiol-3,17-O,O-bis-sulphamate and 2-deoxy-D-glucose in combination: A potential treatment for breast and prostate cancer. Br J Cancer 99:1842–1848.

Tophkhane C, Yang S, Zhao ZJ, Yang X. 2009. Cell density-dependent regulation of p73 in breast cancer cells. Int J Oncol 35:1429–1434.

Vardimon L, Fox LL, Degenstein L, Moscona AA. 1988. Cell contacts are required for induction by cortisol of glutamine synthetase gene transcription in the retina. PNAS USA 85:5981–5985.

Vinci M, Gowan S, Boxall F, Patterson L, Zimmermann M, Court W, Lomas C, Mendiola M, Hardisson D, Eccles SA. 2012. Advances in establishment and analysis of three-dimensional tumor spheroid-based functional assays for target validation and drug evaluation. BMC Biol 10:29.

Xia X, Yang J, Li F, Li Y, Zhou X, Dai Y, Wong ST. 2010. Image-based chemical screening identifies drug efflux inhibitors in lung cancer cells. Cancer Res 70:7723–7733.

Xu X, Sabanayagam CR, Harrington DA, Farach-Carson MC, Jia X. 2014. A hydrogel-based tumor model for the evaluation of nanoparticle-based cancer therapeutics. Biomaterials 35:3319–3330.

Zellmer VR, Zhang S. 2014. Evolving concepts of tumor heterogeneity. Cell Biosci 4:69.

Zhou Y, Arai T, Horiguchi Y, Ino K, Matsue T, Shiku H. 2013. Multiparameter analyses of three-dimensionally cultured tumor spheroids based on respiratory activity and comprehensive gene expression profiles. Anal Biochem 439:187–193.